Numerical Study of Blended Winglet Geometry Variations on Unmanned Aerial Vehicle Aerodynamic Performance

Fungky Dyan Pertiwi*, Arif Wahjudi

Department of Mechanical Engineering, Institut Teknologi Sepuluh Nopember, Surabaya 60111, Indonesia

Abstract

An unmanned aerial vehicle (UAV) is an unmanned aircraft that can be controlled remotely or flown automatically. Nowadays, the use of UAVs is extensive, not only limited to the military field but also in civilian tasks such as humanitarian search and rescue (SAR) tasks, railroad inspections, and environmental damage inspections. Therefore, study on UAV becomes essential to answer the challenges of its increasingly widespread use. This study explored the addition of a blended winglet on the swept-back wing of the UAV. It was to predict the effect of the aerodynamic performance. The backpropagation neural network (BPNN) method helped to predict the aerodynamic performance of the UAV in the form of a lift-drag coefficient ratio (C_L/C_D) and drag coefficient at 0° angle of attack (C_{D0}). It was based on blended winglet parameters such as height, tip chord, and cant angle. The obtained BPNN modeling has a network architecture of 3 inputs, 2 hidden layers, and 1 output with a mean square error (MSE) of 4.9462e-08 and 4.4756e-06 for the relationships between blended winglet parameters with C_L/C_D and C_{D0}, respectively.

Keywords: unmanned aerial vehicle, backpropagation neural network, tip chord, cant angle, height blended winglet

1. Introduction

UAV is an unmanned flying robot that can be controlled remotely to carry out special missions. UAVs can operate on arduous or dangerous tasks because UAVs have high mobility, good security, and low cost [1]. The UAV operates at subsonic speeds, has limited range, and flies at a certain altitude. The speed of the UAV used other than for military purposes is 10-50 m/s [2]. The use of UAVs is limited to the military and defense fields. It extends to various fields, including traffic control, natural disaster management, infrastructure inspection, law enforcement, agriculture, and wireless coverage [1,3].

The main product of the UAV is its aerodynamic performance. One thing that hinders aerodynamic performance when the UAV is in flight is vortices. Vorticity is a phenomenon that results from the lift force of the aircraft. This phenomenon is unavoidable and is considered a side effect of the aircraft's forces. The vortices are responsible for the induced drag [4]. Induced drag is a phenomenon that occurs at the wingtip in three dimensions which can be explained by the Prandtl lifting line theory [5]. Induced drag accounts for 30% of the total drag force [4]. One way to reduce induced drag is to place the vertical surfaces on the aircraft's wingtips. Lanchester long investigated this research in 1897; in addition to reducing the induced drag on the wing, the vertical surface

also improves the wing's aerodynamic performance [6]. The vertical surface on the wing is better known as the winglet. The function of the winglet is to reduce the trailing vortex due to high-pressure airflow under the wing to low pressure above the wing [7]. Several studies have stated that winglets can reduce the drag coefficient and increase the lift coefficient [8,9]. In addition to improving aerodynamic performance, the provision of winglets also proves an increase in aircraft flight time by 10% [10].

The wingtip design is inseparable from the parameters that make the wingtip have different shapes. Whitcomb first introduced the wingtip parameters, namely sweep, cant, taper, and toe-out angle on the upper winglet. Lower winglet with outward cant and toe-in [6]. One form of the winglet is often known as the blended winglet, which is a modification of the rectangular winglet. The winglet geometry is designed based on the aircraft's operating range and the intended purpose. P. Panagiotou et al. investigated six configurations of blended winglet parameters, namely height, cant angle, and tip chord with PSU airfoils. The research aims to design winglets to improve aerodynamic performance and flight endurance [10]. Mark D. Maughmer designed winglets for low-speed aircraft with several winglet parameters: area, height, cant angle, sweep angle, twist angle, and toe angle. Parameter determination is done uniquely to achieve the expected

---

performance [11]. Jacob R. Weierman has used winglet geometries including height, angle of cant, radius, twist, sweep, root chord, tip chord to optimize UAVs with minimum induced drag [12]. Tjahjana et al. have used cant angle and taper ratio (comparison of tip chord – root chord winglet) to improve the aerodynamic performance of the Micro UAV [13]. Research on UAVs with blended winglets found that C_L/C_D increased by 15.61%, 4.1%, and 22%, while drag decreased by 5% and 2.8% [12,14,15]. Wingtip analysis is also developed using an algorithm to find the optimal winglet factor. The aerodynamic optimization method by combining artificial neural network (ANN) and genetic algorithm (GA) is mixed and matched with CFD (computational fluid dynamic) and XFLR5 simulations. The purpose of the combination is to find the optimal design of the existing parameters [16].

Based on the literature review, the current study is motivated to predict aerodynamic performance (ratio of lift coefficient – drag coefficient and drag coefficient at zero degrees angle of attack) by evaluating three parameters of the winglet: height, tip chord, and cant angle. These three parameters were often used in winglet design research to improve aerodynamic performance and the limitations of XFLR5 in the UAV winglet design, so they were selected for optimization. A numerical study of three parameters was carried out to find the aerodynamic value of the UAV using XFLR5. A Matlab 2019b helps backpropagation neural network (BPNN) simulation predict and evaluate the parameters with mean square error (MSE) as output. Other outputs, namely BPNN prediction graph and surface graph, are used to clarify the relationship of the three parameters to the aerodynamic performance of the UAV.

2. Method

Figure 1 shows a winglet geometry with three design parameters: height (h), tip chord (Ct), and cant angle (Λ). The range of parameter values is shown in Table 1. Each parameter had four different variations. The height and tip chord values referred to the Whitcomb (upper winglet) geometry [6], namely h=Ct and Ct=0.21 of wing tip chord. Later on, refs. [10, 17]indicated that the cant angle to improve aerodynamic performance was not more than 90°.

The winglet design was put on the wing with root chord 189 mm, tip chord 160 mm, wing offset 93 mm, wing length 400 mm, the blend radius 10 mm from the wing length. This study used the Cal2263m airfoil, the recommended airfoil for small unmanned aerial vehicles [18]. Full factorial randomization of three parameters with four variations resulted in 64 data without replication. Then, numerical analysis was carried out using the XFLR5 program from the data. XFLR5 used the XFOIL code for the aerodynamic performance analysis of 2D airfoils. This program could calculate lift, drag, pitching moment, pressure coefficient, and aircraft stability by combining the viscous/inviscid and panel methods [19]. XFLR5 only analyzed the wing, not the entire body or rear tail wing, so the program provided fast and inexpensive data, but the UAV's goal was to fly effectively [20]. The initial analysis in this program was a numerical analysis of the 2D airfoil, which produced aerodynamic values for the airfoil used. Next, the wing and plane were designed with polar type I (fix speed) 22.22 m/s, analyzed using ring vortex (VLM2) and 4992 VLM panels. The output of this program consisted of C_L and C_D values in the specified angle of attack range (-1.5°to 11.5°) so that C_L/C_D values could be calculated and C_{D0} is observed. This response monitored the UAV in cruising flight conditions, as shown in Figure 2.

Analysis of variance (ANOVA) testing with a confidence interval of 95% was carried out to prove the relationship between aerodynamic values and parameters. Furthermore, the output data was used as the target data for the BPNN simulation. A preliminary step in the BPNN simulation was to normalize the target data to a dimensionless value with a range of -1 to 1. The activation function used to connect the input to the hidden layer was *tansig*, and the hidden layer to the output was *purelin*. Selected two hidden layers and a maximum of 15 neurons in each layer with a training function, Lavenberg Marquardt (*trainlm*) [16]. Data for BPNN was divided into three randomly, namely 70% training data, 15% validation data, and 15% testing data. The BPNN network structure formed from training between layers and the activation function was reasonable concerning the MSE value [21,22]. The training process stopped if the smallest MSE was generated and MSE was stored.

(a) Z-view.　　　　　　　　**(b)** X-view.
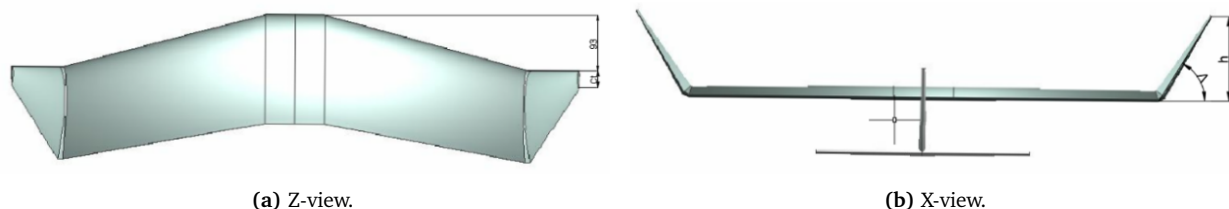
Figure 1. Blended winglet geometry in XFLR5.

Table 1. Variation of blended winglet geometry.

	Unit	Variation			
		1	2	3	4
Height (h)	mm	125	145	155	160
Tip Chord (Ct)	mm	18	22	28	33
Cant angle (Λ)	°	60	70	80	90
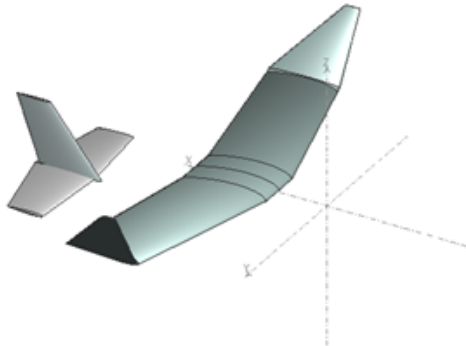
Figure 2. UAV design with XFLR5

The process above is followed by making a solid cylinder with diameter of 1 mm and length of 24.96 mm. The previously made 2D sketch is then wrapped onto the cylinder, using a deboss of 0.08 mm on the cylinder as the thickness of the stent. Then, the debossed cylinder are extrude cut by a circle with a radius of 0.42 mm to remove the cylinder's center part. The final geometry are shown in Figure 2.

3. Results and Discussion

3.1. Training C_L/C_D

BPNN forecasting for C_L/C_D targets resulted in a 3-6-3-1 network with MSE 4.9462e-08. In the BPNN process, the first hidden layer with the sigmoid hyperbolic tangent function (*tansig*) produced weight ($b1$) and bias ($LW1_1$) output through Equation (1). The second hidden layer, tansig, created weight ($b2$) and bias ($LW2_1$) through Equation (3). Output layer with purelin function produced weight ($b3$) and bias ($LW3_2$) through Equation (6).

$$a1 = tansig(LW1_1 \cdot Xp1 + b1)$$
$$= \frac{2}{(1 + exp[-2(LW1_1 \cdot Xp1 + b1)] - 1)} \quad (1)$$

$$b1 = \begin{vmatrix} -4.1534 \\ -0.4330 \\ -1.0925 \\ 0.7784 \\ 0.2069 \\ 3.8073 \end{vmatrix} \quad (2)$$

$$LW1_1 = \begin{vmatrix} 0.5596 & 0.04466 & 1.1773 \\ -0.0357 & -0.0093 & -0.2354 \\ 0.0963 & -0.2170 & -0.4878 \\ -2.2225 & 0.01590 & -0.0701 \\ -0.0224 & 0.00564 & 0.2398 \\ 0.9449 & -0.0711 & 0.9429 \end{vmatrix}$$

$$a2 = tansig(LW2_1 \cdot a1 + b2)$$
$$= \frac{2}{(1 + exp[-2(LW2_1 \cdot a1 + b2)] - 1)} \quad (3)$$

$$b2 = \begin{vmatrix} -0.9655 \\ -0.5626 \\ -1.6974 \end{vmatrix}$$

$$LW1_1 = \begin{vmatrix} 1.0826 & -0.5274 & 0.8150 \\ 0.6447 & -1.8516 & 0.1186 \\ 0.4264 & -0.7921 & -0.8642 \\ -0.0162 & 1.3071 & 1.2319 \\ -0.0498 & -2.7280 & 0.0525 \\ 0.0421 & 1.6183 & 0.4537 \end{vmatrix} \quad (4)$$
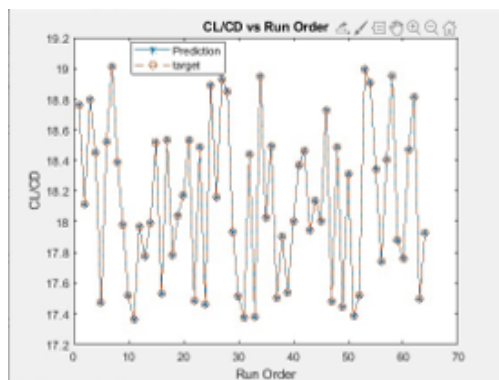
(a) C_L/C_D.
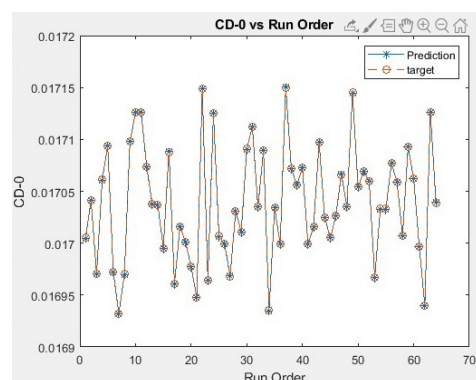
(b) C_{D0}.

Figure 3. Prediction of ANN and targets.

(a) C_L/C_D.

(b) CC_{D0}
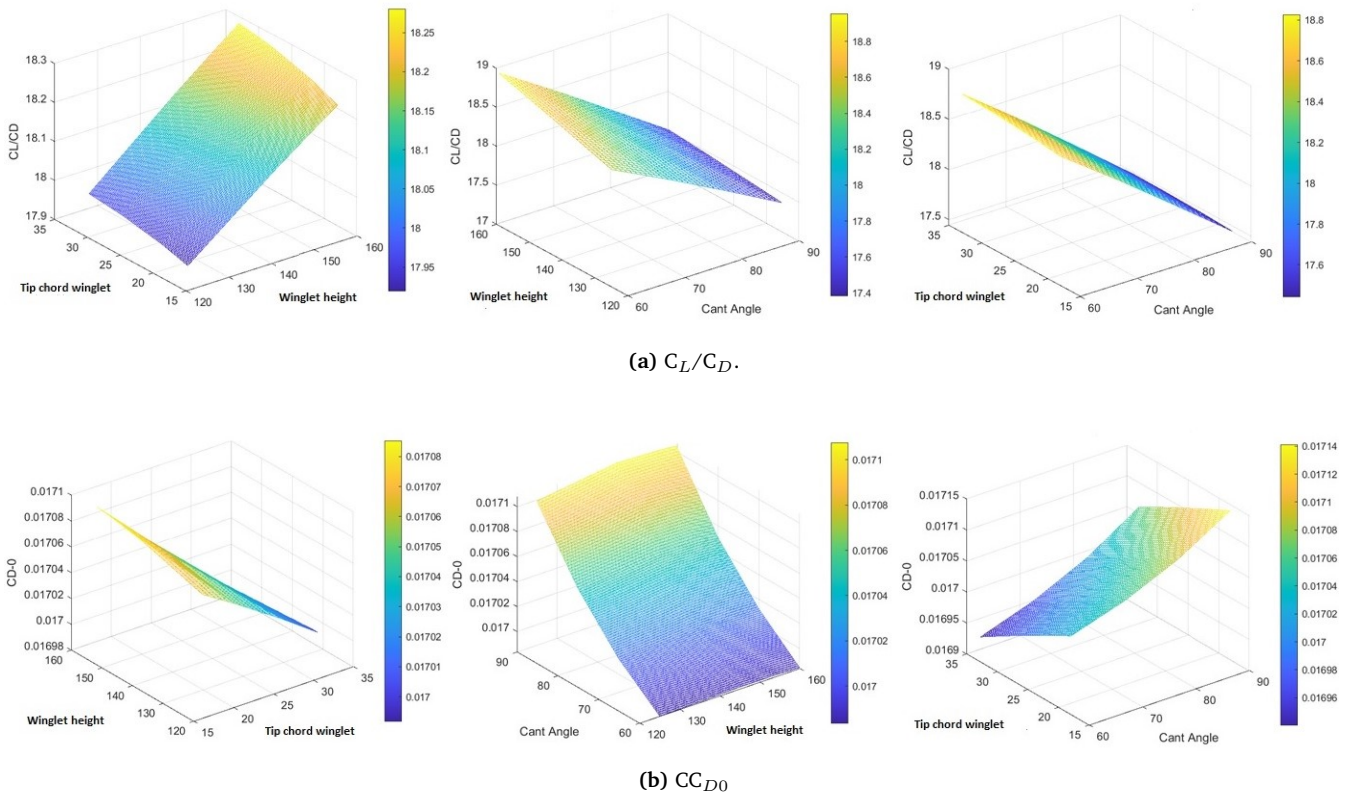
Figure 4. Graph of the relationship between the blended winglet parameters and aerodynamic performance.

$$a2 = purelin(LW3_2 \cdot a2 + b3) \\ = LW3_2 * a2 + b3 \quad (5)$$

$$b3 = \begin{vmatrix} 0.3378 \end{vmatrix}$$
$$LW3_1 = \begin{vmatrix} -2.6444 & 3.2169 & -0.1963 \end{vmatrix} \quad (6)$$

Figures 3(a) and 3(b) show the BPNN prediction graph. The validation used the error value (difference between experimental and predicted results) from BPNN [22]. In this study, the data from the numerical analysis of XFLR5 was compared with that output. The testing data used 15% of the overall data taken randomly, so there were ten validation data. In the C_L/C_D response, the average error value was 0.000699%, and the average error value for the C_{D0} response is 0.00105%. The error value produced by the two responses was 5% smaller; this indicated that the prediction made by BPNN was good.

3.2. Training C_{D0}

The results of BPNN forecasting for the C_{D0} response had the same process as the C_L/C_D response. However, the C_{D0} response in the BPNN resulted in a 3-3-8-1 network and an MSE value of 4.4756e-06. The calculation process for each hidden layer used Equations (1), (3), (5), while the weight and bias values were shown by Equations (7)-(10).

$$b1 = \begin{vmatrix} -0.3156 \\ -0.0397 \\ -0.0864 \end{vmatrix} \quad (7)$$

$$b2 = \begin{vmatrix} 1.7185 \\ 1.7853 \\ -0.4805 \\ 2.5329 \\ -3.2006 \\ 1.2513 \\ -2.6162 \\ 0.4017 \end{vmatrix} \quad (8)$$

$$LW2_1 = \begin{vmatrix} 1.8472 & 2.6492 & -2.0555 \\ 1.1307 & 2.9307 & 2.6012 \\ 3.2131 & 3.9617 & 2.6740 \\ -0.5915 & -2.7753 & -0.6868 \\ -3.4106 & 0.5088 & 2.2847 \\ 0.0158 & 2.3182 & 3.3871 \\ -1.9353 & -0.7017 & 0.3316 \end{vmatrix}$$

$$b3 = \begin{vmatrix} 0.3769 \end{vmatrix} \quad (9)$$

$$b3 = \begin{vmatrix} -0.1635 & -0.1258 & -0.6434 & 0.4652 \\ -0.7183 & -1.9356 & 1.95137 & 2.9877 \end{vmatrix} \quad (10)$$

3.3. Training result

Figure 4(a) shows the relationship of three blended winglet parameters to the C_L/C_D response. The range of response values obtained was 17.38 to 18.95. Three parameters indicated that a considerable parameter value increased the C_L/C_D value. However, the parameter that had the most substantial influence was the cant angle. Based on the image, the cant angle combined with the height and tip chord parameters resulted in a C_L/C_D value of 18.83 to 18.95. The C_{D0} response is shown in Figure 4(b), with the minimum C_{D0} value being 0.01694. The parameter that strongly influenced the decrease in C_{D0} was the cant angle, which produced a value of 0.01694 to 0.01698 with a combination of tip chord parameters and height.

Figure 4 also showed that the effect of winglet height could improve the aerodynamic performance of the UAV. The high value equal to the wing tip chord length (maximum size) enhanced the aerodynamic performance of the aircraft [6, 23]. The increase in winglet height also had a drawback in the aircraft load, where the bending moment of the plane increased with increasing length [6]. Regarding the decrease in C_L/C_D, XFLR5 or the panel method could not be used to predict viscous drag and stall accurately. Further research is needed to determine the weight of the structure and the decrease C_L/C_D value due to the increase in winglet height.

4. Conclusion

The MSE generated by BPNN for C_L/C_D was 4.9462e-08, while for C_{D0} was 4.4756e-06. In addition to MSE, BPNN produced a prediction graph. Through the prediction graph, it can be stated that the training is qualitatively good. The surface graph created a meaningful relationship between the parameters and the response. The most significant influence of the parameters on the chart with the height and cant angle parameters on the increase of C_L/C_D was the cant angle. Meanwhile, the factor affecting the relationship between the tip chord and the cant angle was the cant angle parameter.

References

[1] M. N. Boukoberine, Z. Zhou, and M. Benbouzid, "A critical review on unmanned aerial vehicles power supply and energy management: Solutions, strategies, and prospects," *Applied Energy*, vol. 255, p. 113823, 2019.

[2] S. H. S. Putro, *Studi aerodinamika shifted downstream winglet untuk wing airfoil eppler 562 pada unmanned aerial vehicle*. PhD thesis, Institut Teknologi Sepuluh Nopember, 2019.

[3] A. S. Saeed, A. B. Younes, C. Cai, and G. Cai, "A survey of hybrid unmanned aerial vehicles," *Progress in Aerospace Sciences*, vol. 98, pp. 91–105, 2018.

[4] F. Catalano and H. Ceron-Muñoz, "Experimental analysis of aerodynamics characteristics of adaptive multi-winglets," in *43rd AIAA Aerospace Sciences Meeting and Exhibit*, p. 1231, 2005.

[5] L. Zhang, M. Dongli, Y. Muqing, and W. Shaoqi, "Optimization and analysis of winglet configuration for solar aircraft," *Chinese Journal of Aeronautics*, vol. 33, no. 12, pp. 3238–3252, 2020.

[6] R. T. Whitcomb, "A design approach and selected wind tunnel results at high subsonic speeds for wingtip mounted winglets," tech. rep., 1976.

[7] H. Putro, S. Sutardi, and A. Wawan, "Numerical study of aerodynamic analysis on wing airfoil naca 43018 with the addition of forward and rearward wingtip fence," in *Proceedings of the International Mechanical Engineering and Engineering Education Conferences*, 2016.

[8] A. Hossain, A. Rahman, J. Hossen, P. Iqbal, N. Shaari, and G. Sivaraj, "Drag reduction in a wing model using a bird feather like winglet," *Jordan Journal of Mechanical and Industrial Engineering*, vol. 5, no. 3, 2011.

[9] A. Hossain, P. Arora, A. Rahman, A. Jaafar, A. Iqbal, and M. Ariffin, "Lift analysis of an aircraft model with and without winglet," in *7th International Conference on Mechanical Engineering, ICME*, pp. 28–30, 2007.

[10] P. Panagiotou, P. Kaparos, and K. Yakinthos, "Winglet design and optimization for a male uav using cfd," *Aerospace Science and Technology*, vol. 39, pp. 190–205, 2014.

[11] M. Maughmer, "The design of winglets for low-speed aircraft," *Technical Soaring*, vol. 30, no. 3, p. 6173, 2006.

[12] J. Weierman and J. Jacob, "Winglet design and optimization for uavs," in *28th AIAA Applied Aerodynamics Conference*, p. 4224, 2010.

[13] D. D. D. P. Tjahjana, I. Yaningsih, B. Y. L. Imama, and A. R. Prabowo, "Aerodynamic performance enhancement of wing body micro uav employing blended winglet configuration," 2021.

[14] A. Rajesh, D. M. G. Prasad, and A. Praveen, "Design and analysis of ucav wing with a winglet by varying the cant angle," *International Journal of Engineering Research & Technology (IJERT), ISSN*, pp. 2278–0181, 2015.

[15] S. Kontogiannis, D. Mazarakos, and V. Kostopoulos, "Atlas iv wing aerodynamic design: From conceptual approach to detailed optimization," *Aerospace Science and Technology*, vol. 56, pp. 135–147, 2016.

[16] A. Boutemedjet, M. Samardžić, L. Rebhi, Z. Rajić, and T. Mouada, "Uav aerodynamic design involving genetic algorithm and artificial neural network for wing preliminary computation," *Aerospace Science and Technology*, vol. 84, pp. 464–483, 2019.

[17] A. Hossain, A. Rahman, J. Hossen, A. Iqbal, and S. Hasan, "Application of fuzzy logic approach for an aircraft model with and without winglet," *International Journal of Mechanical, Industrial and Aerospace Engineering*, vol. 4, no. 2, pp. 78–86, 2010.

[18] N. K. Hieu and H. T. Loc, "Airfoil selection for fixed wing of small unmanned aerial vehicles," in *AETA 2015: Recent Advances in Electrical Engineering and Related Sciences*, pp. 881–890, Springer, 2016.

[19] İ. H. GÜZELBEY, Y. ERASLAN, and M. H. DOĞRU, "Numerical investigation of different airfoils at low reynolds number in terms of aerodynamic performance of sailplanes by using xflr5," *Karadeniz Fen Bilimleri Dergisi*, vol. 8, no. 1, pp. 47–65, 2018.

[20] A. Schumacher, E. Sjögren, and T. Persson, "Winglet effect on induced drag for a cessna 172 wing," 2014.

[21] J. D. Kechagias, A. Tsiolikas, M. Petousis, K. Ninikas, N. Vidakis, and L. Tzounis, "A robust methodology for optimizing the topology and the learning parameters of an ann for accurate predictions of laser-cut edges surface roughness," *Simulation Modelling Practice and Theory*, vol. 114, p. 102414, 2022.

[22] T. D. Salamoni and A. Wahjudi, "Injection molding process modeling using back propagation neural network method," in *AIP Conference Proceedings*, vol. 1983, p. 040009, AIP Publishing LLC, 2018.

[23] S. Setyo Hariyadi, W. A. Widodo, B. J. Pitoyo, *et al.*, "Numerical study of the wingtip fence on the wing airfoil e562 with fence height variations," in *Proceedings of the 6th International Conference and Exhibition on Sustainable Energy and Advanced Materials*, pp. 367–376, Springer, 2020.